

Dead-time Compensation Method for Bus-clamping Modulated Voltage Source Inverter

Reza Asrar Ghaderloo, *Student Member, IEEE*, Yidi Shen, *Student Member, IEEE*,
Chanaka Singhabahu, *Student Member, IEEE*, Rakesh Resalayyan, *Member, IEEE*
and Alireza Khaligh, *Senior Member, IEEE*

Maryland Power Electronics Laboratory, Department of Electrical and Computer Engineering
and The Institute for Systems Research, University of Maryland, College Park, MD 20742 USA
E-mail: rezasarar@umd.edu, yidishen@umd.edu, chanaka@umd.edu,
rakeshr@umd.edu, khaligh@umd.edu; URL: <https://khaligh.umd.edu/>

Abstract—Bus-clamping Pulse Width Modulation (PWM) is an effective method to reduce the switching loss in a three-phase voltage source inverter (VSI). In bus-clamping PWM scheme, the phase legs are switched using high frequency PWM signals for two-third of the line cycle, while for the remaining duration of cycle, the pole voltage is clamped to either positive or negative rail of the DC bus. In PWM operation of a half bridge, a dead-time is applied between the gate signals of complementary switches to ensure safe and reliable operation. However, introduction of dead-time leads to poor power quality, increased Total Harmonic Distortion (THD) and variation in actual voltage compared to the intended pole voltage. Moreover, when the bus-clamping technique is used, the PWM has both high frequency switching region and clamped region in a line cycle, and consequently, the undesired effects of dead-time are further aggravated. Therefore, in order to enhance the quality of output voltage, this paper presents a dead-time compensation strategy for a VSI operating with bus-clamping PWM. The proposed method calculates the required compensation term to be added on the modulation signal considering wide range of operating conditions. Additionally, the compensation includes a new strategy for low current conditions near zero-crossing to avoid distortion. The proposed method is verified by simulation and experiments in a three-phase VSI with a switching frequency of 100 kHz and a fundamental frequency of 60Hz.

Index Terms—Voltage Source Inverter, Pulse-width Modulation, Dead-time, Bus-clamping

I. INTRODUCTION

Two-level voltage source inverter (VSI) is a widely used topology to generate three phase sinusoidal output voltage due to its low device count, ease of modulation and well-established literature [1], [2]. Three phase VSI consists of three half-bridge legs, with each leg being modulated with complimentary pulses with a dead time between the gate signals of the switches [3], [4]. While dead-time is a necessity for VSI, it introduces undesired distortion at the output of VSI [5], [6]. Although the use of wide band-gap devices with fast transition speed can minimize the required dead-time [7], operation at high switching frequencies still accumulates the dead-time effect and distorts the output voltage. Hence, the effects of dead-time should be investigated in the case of a practical VSI.

There are several existing methods for dead-time compensation [3], [5], [8]–[11]. In [3], the dead-time effect is

compensated directly by a closed-loop controller design for output waveform. Since the dead-time will affect the output by introducing odd harmonics, the feedback controller is designed to regulate the induced harmonics in [5] and [8]. The main constraint of this method is the demand for high gain and high bandwidth control. In feed-forward type dead-time compensation method, the compensation voltage is derived based on current value and direction, then added to the modulation signal [9]. To eliminate the sampling delays in current sensing and to improve the dead-time compensation accuracy, predicted phase current is used in [10], however, the precise parameters of inverter load are required in this method.

Emergence of wide band-gap semiconductors has pushed the switching frequencies from a few kilo-Hertz to 100kHz–500kHz for VSIs with power rating of 1kW to 3kW [8], [12]. Although the higher switching frequencies bring up benefits in lower converter volume and faster dynamic response, it imposes new challenges including aforementioned dead-time effect [9]. Another known challenge in higher switching frequency is increased switching losses. Researchers have investigated various methods to reduce the switching loss in three phase VSI such as bus-clamping modulation [11]. The above-mentioned works have studied dead-time compensation in regular sine-wave modulated VSI, whereas the dead-time compensation in the case of bus-clamping PWM has not been well-investigated.

In this paper, a novel method is proposed to compensate the dead-time effect in bus-clamping modulated VSI based on sensed load current. Section II includes the analysis of dead time effect and calculation of compensation voltage based on load current. In Section III, the dead time compensation method is extended to bus-clamping modulation considering the sampling delay for current sensing. Subsequently in Section IV, experimental results are presented to validate the proposed method. Finally, the Section V concludes the paper.

II. THE ANALYSIS OF DEAD-TIME EFFECT

The basic structure of a VSI half-bridge leg is shown in Fig. 1 where an inductor represents either the output filter or an inductive load. The six operating modes of a half bridge in

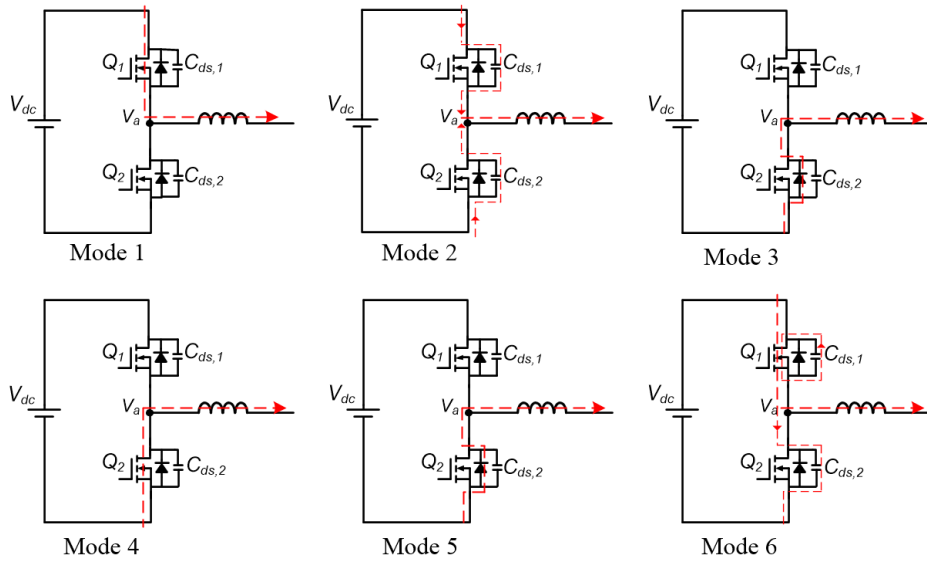


Fig. 1. Operating modes of a half bridge in one switching cycle.

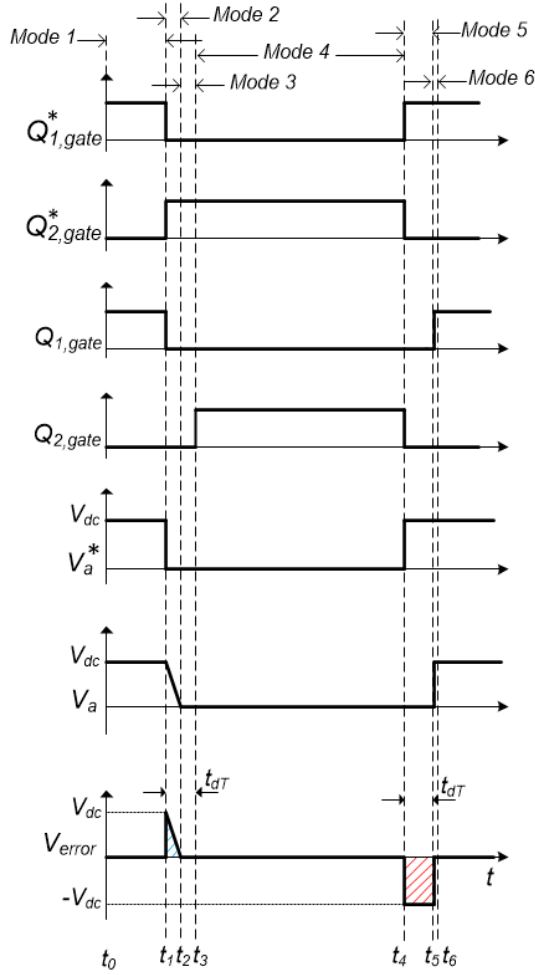


Fig. 2. Waveforms of half bridge for a switching cycle considering positive current direction.

one switching cycle assuming positive direction for inductor current (phase current drawn out of the pole) is depicted in Fig. 1. Fig. 2 illustrates gating and pole voltage waveforms of the half bridge, showing the effect of dead-time and drain-to-source parasitic capacitance ($C_{ds,1}, C_{ds,2}$). In this analysis, $C_{ds,1}$ and $C_{ds,2}$ are assumed to be constant. In Fig. 2, the $Q_{1,gate}^*$ and $Q_{2,gate}^*$ are ideal gate signals and V_a^* is the ideal pole voltage without dead-time. While, $Q_{1,gate}$ and $Q_{2,gate}$ are the gate signals and V_a is the actual pole voltage after applying the dead-time. V_{error} is the error voltage which is added to the ideal pole voltage due to dead-time and C_{ds} parasitic capacitor effects, and t_{dT} is the time duration of dead-time.

The description for each mode of operation is given below:

Mode 1 ($t_0 - t_1$): In the first mode, the Q_1 switch is ON and the load current is flowing through its channel. In this mode, the pole voltage is equal to V_{dc} . The voltage across $C_{ds,1}$ is zero and voltage across $C_{ds,2}$ capacitor is V_{dc} . This mode ends by turning off the gate of switch Q_1 at t_1 .

Mode 2 ($t_1 - t_2$): In this mode, the current in Q_1 channel is ceased and the load current is comprised of current through $C_{ds,1}$ and $C_{ds,2}$ capacitors (as shown in Fig. 2). During this mode, the $C_{ds,1}$ capacitor is gradually charged to V_{dc} and $C_{ds,2}$ capacitor is discharged to zero. Hence, in this interval, the pole voltage V_a is gradually decreased from V_{dc} to zero. This mode ends at t_2 when pole voltage reaches zero. It should be noted that, if the load current magnitude is larger or C_{ds} capacitor value is smaller, the time interval for this mode ($t_1 - t_2$) would be shorter. In Fig. 2, the magnitude of load current is assumed to be high enough to completely charge $C_{ds,1}$ and discharge $C_{ds,2}$ before triggering Q_2 .

Mode 3 ($t_2 - t_3$): At t_2 , the $C_{ds,1}$ is charged to V_{dc} and $C_{ds,2}$ capacitor is completely discharged, thus, the load current flows through the anti-parallel diode of switch Q_2 . This mode ends at $t = t_3$ when the Q_2 switch is triggered. It should be noted that the time interval between t_1 and t_3 is when the

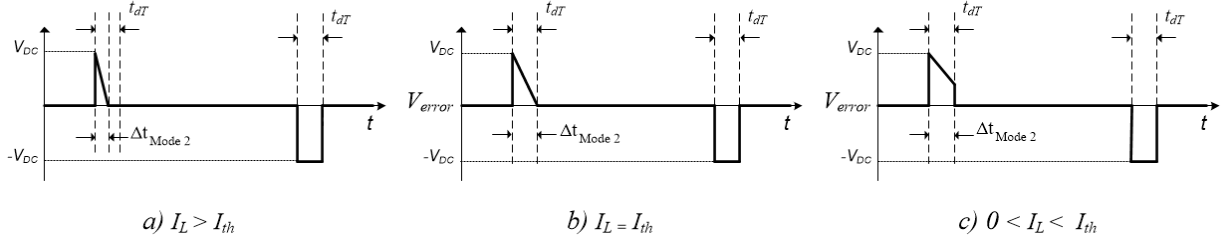


Fig. 3. Three types of error voltage waveforms based on magnitude of inductor current for positive current direction.

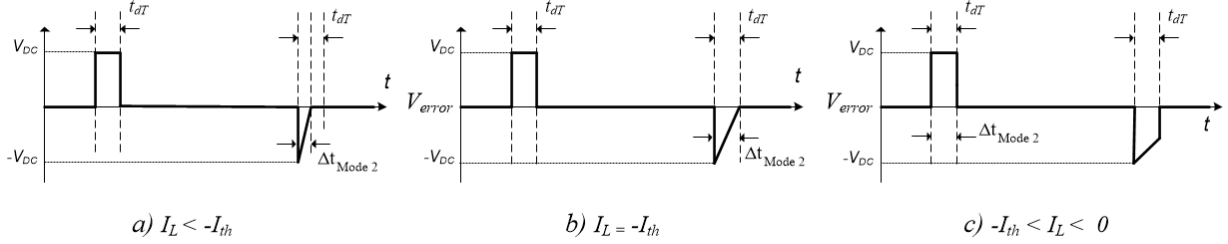


Fig. 4. Three types of error voltage waveforms based on magnitude of inductor current for negative current direction.

dead-time is applied.

Mode 4 ($t_3 - t_4$): At $t = t_3$, the gate signal is applied to Q_2 switch and load current transfers from anti-parallel diode of Q_2 to its channel. This mode continues until gate signal is removed from Q_2 switch.

Mode 5 ($t_4 - t_5$): Once the gate signal is removed from Q_2 switch, the load current flows through Q_2 anti-parallel diode once more. This mode ends at $t = t_5$ when the Q_1 switch is triggered.

Mode 6 ($t_5 - t_6$): At $t = t_5$, the Q_1 switch turns on. Once Q_1 starts to conduct, the capacitor $C_{ds,1}$ discharges into Q_1 channel. Concurrently, current passes through Q_1 channel towards capacitor $C_{ds,2}$ to charge it to V_{dc} . Since the current discharging $C_{ds,1}$ and charging $C_{ds,2}$ capacitor is high in magnitude, the time interval for mode 6 is assumed to be negligible. During this mode, the Q_1 channel provides the load current, discharge current of $C_{ds,1}$ capacitor and charge current of $C_{ds,2}$ capacitor.

As shown in Fig. 2, for positive current direction of inductor, there is a rectangle-shape (red shadowed) negative voltage error due to dead-time effect and a triangle-shape (blue shadowed) positive voltage error due to C_{ds} capacitors. Hence, in each switching cycle, an error voltage is introduced to the intended pole voltage which results in distortion and voltage drop.

Based on the analysis of Mode 2 operation above, since the load current is charging and discharging the C_{ds} capacitors, the time duration of Mode 2, Δt_{Mode2} , is calculated in (1) and (2).

$$I_L = 2C_{ds} \frac{V_{dc}}{\Delta t_{Mode2}} \quad (1)$$

$$\Delta t_{Mode2} = t_2 - t_1 = \frac{2C_{ds}V_{dc}}{I_L} \quad (2)$$

In (1) and (2), V_{DC} is the DC-link voltage and I_L is the inductor current. Based on (2), Δt_{Mode2} is inversely proportional to inductor current. From the mode-wise operation analysis above, the maximum value of Δt_{Mode2} is equal to dead-time duration, t_{dT} . Hence, based on the magnitude of inductor current, three types of error voltage waveforms are obtained for positive current direction as shown in Fig. 3.

In Fig. 3(a), referring to mode 2 of half bridge operation analysis, the inductor current is large enough (above certain threshold current I_{th}) to complete charging of $C_{ds,1}$ capacitor and discharging of $C_{ds,2}$ capacitor before triggering Q_2 switch, thus, Δt_{Mode2} is less than dead-time and it can be obtained from (2). In Fig. 3 (b), the process of charging the $C_{ds,1}$ capacitor and discharging the $C_{ds,2}$ capacitor is completed at the instant of triggering the Q_2 switch. Hence, Δt_{Mode2} is equal to dead-time. Based on (2), this threshold current I_{th} is calculated in (3).

$$I_{th} = \frac{2C_{ds}V_{dc}}{t_{dT}} \quad (3)$$

In Fig. 3 (c), the magnitude of inductor current is smaller than I_{th} , thus, it will take longer than t_{dT} to fully charge the $C_{ds,1}$ capacitor and discharge the $C_{ds,2}$ capacitor in dead-time interval. Therefore, the error voltage due to C_{ds} capacitors effect has a trapezoidal shape.

With similar analysis, possible error voltage waveforms for negative direction of current are shown in Fig. 4 .

Based on possible error voltage waveforms for positive and negative current directions, the average of error voltage in one

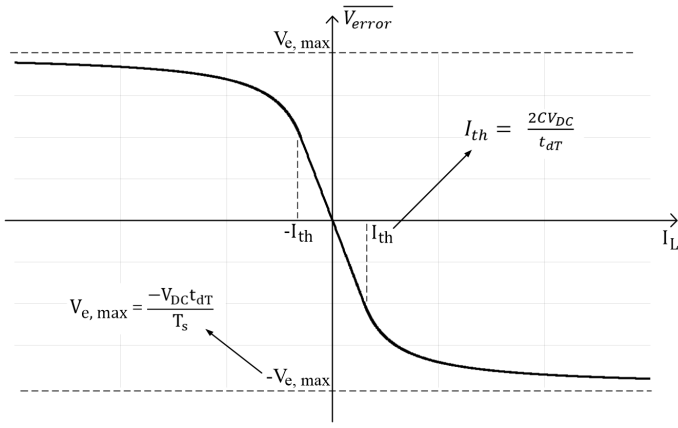


Fig. 5. The switching cycle average of error voltage due to dead-time and C_{ds} capacitors effects as a function of current.

switching cycle can be determined as (4).

$$\overline{V_{error}} = \begin{cases} -\frac{V_{DC}t_{dT}}{T_s} + \frac{C_{ds}V_{DC}^2}{I_L T_s}, & I_{th} \leq I_L \\ -\frac{t_{dT}^2 I_L}{4C_{ds}T_s}, & -I_{th} < I_L < I_{th} \\ \frac{V_{DC}t_{dT}}{T_s} - \frac{C_{ds}V_{DC}^2}{I_L T_s}, & I_L \leq -I_{th} \end{cases} \quad (4)$$

According to (4), the average of error voltage ($\overline{V_{error}}$) due to dead-time and C_{ds} capacitors effects, which is added to ideal pole voltage is plotted in Fig. 5.

It is evident from Fig. 5 that $\overline{V_{error}}$ is smooth in the area of current zero-crossing point, thus, the compensation of error will not result in distortion by sudden changes in voltage. However, if the C_{ds} capacitor effect is not considered, sudden changes near current zero-crossing can exist, as in some of the conventional methods [10].

Assuming a sinusoidal switching cycle average pole voltage with lagging power factor, the ideal and actual switching cycle average pole voltage waveforms including dead-time and C_{ds} capacitors effects are shown in Fig. 6.

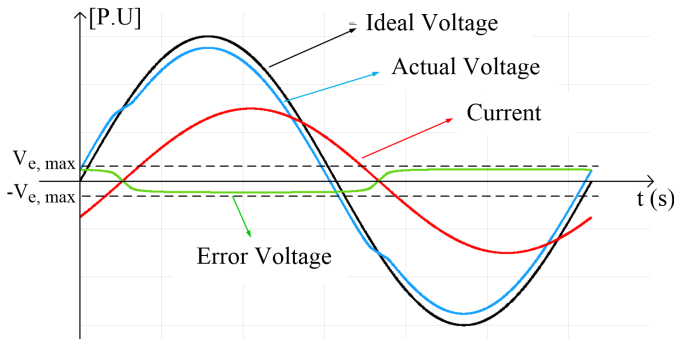


Fig. 6. The ideal and actual switching cycle average pole voltage waveforms including the effects of dead-time and C_{ds} capacitors for sinusoidal PWM.

According to Fig. 6, in positive half cycle of inductor current, the error voltage is negative, whereas, during the

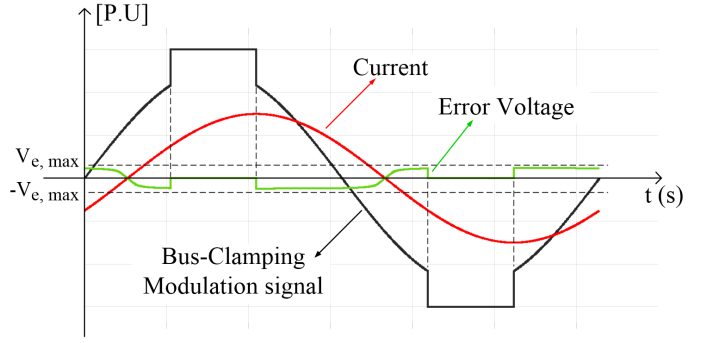


Fig. 7. The modulation signal, current and error voltage waveforms for bus-clamping modulation.

negative half cycle of inductor current, the error voltage is positive.

III. DEAD-TIME COMPENSATION METHOD FOR BUS-CLAMPING PWM

In bus-clamping PWM, each leg will stop switching for one-third of the line cycle [10], hence, during this clamped interval, the error voltage due to dead-time and C_{ds} capacitors effects is zero. Fig. 7 illustrates the $\overline{V_{error}}$ for a VSI half bridge leg which is controlled with bus-clamping modulation.

To compensate the effects of dead-time and C_{ds} capacitors, a signal corresponding to $-\overline{V_{error}}$ is added to the bus-clamping modulation signal. It can be concluded from Fig. 7 that the accuracy of compensation is highly dependent on inductor current direction. However, in practical implementations, there is a propagation delay (T_{delay}) between the sampled and the actual current which leads to reduced accuracy of compensation approach. As shown in (5), this can be addressed with simple current prediction method by adding the ωT_{delay} to the phase of sampled current [10].

$$\begin{cases} i'_a = I_P \sin(\theta_i + \omega T_{delay}) \\ i'_b = I_P \sin(\theta_i - 120^\circ + \omega T_{delay}) \\ i'_c = I_P \sin(\theta_i + 120^\circ + \omega T_{delay}) \end{cases} \quad (5)$$

In (5), I_P is the magnitude, θ_i is the phase and ω is the angular frequency of current which can be calculated according to sampled three-phase current. The i'_a , i'_b and i'_c are the predicted values of current. The T_{delay} can be estimated based on current sensing circuit.

The proposed method is simulated for a three phase VSI controlled with bus-clamping modulation. The specifications of the VSI are tabulated in Table I. The simulated switching cycle average of the pole voltage with and without dead-time is shown in Fig. 8. The voltage distortion is evident from Fig. 8 reflecting the importance of compensating the dead-time and C_{ds} capacitors effects.

In Fig. 9, phase current, error voltage $\overline{V_{error}}$ for sine PWM and bus-clamping PWM, and bus-clamping modulation signal

TABLE I
THE CHARACTERISTICS OF SIMULATED VSI

Design Variable	Value
DC-link voltage	$V_{DC} = 400V$
Switching frequency	100 kHz
Dead-time	$t_{dT} = 200ns$
Switch C_{ds} capacitor	100 pF

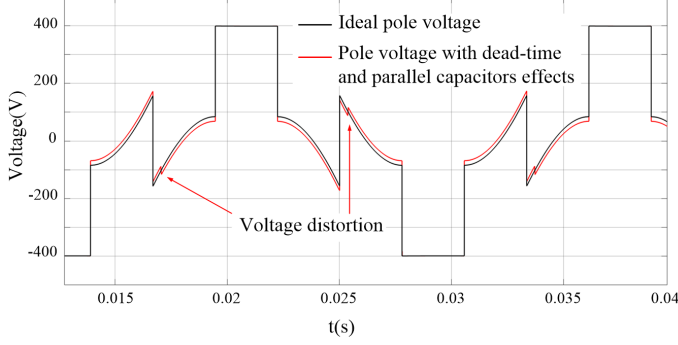


Fig. 8. The average of pole voltage with dead-time (red) and without dead-time (black).

are shown. The $\overline{V_{error}}$ for bus-clamping PWM is set to zero when the modulation signal is clamped to +1 or -1 and is calculated based on (4) when not clamped. The proposed method of compensating the dead-time and C_{ds} capacitors effects is activated by adding $-\overline{V_{error}}/V_{DC}$ to the modulation signal. The resultant average of pole voltage is shown in Fig. 10, where the actual voltage matches the intended voltage by activation of the proposed compensation.

IV. EXPERIMENTAL RESULTS

To verify the operation of proposed method in compensating the effects of dead-time and C_{ds} capacitors, a three-phase VSI hardware prototype is built, as shown in Fig. 11. The key parameters of prototype circuit are tabulated in Table II. To highlight the effect of dead-time on output voltage, the dead-time is set to 300ns.

Based on commanded bus-clamping modulation index of $m=0.808$ to VSI, the desired output line-to-line voltage is expected to be 173Vrms ($V_{ph}=100$ Vrms) as shown in (6). However, as shown in Fig. 12(a), the output voltage is dropped to 167Vrms due to the effects of dead-time and C_{ds} capacitors.

$$V_{ph,rms} = \frac{mV_{dc}}{2\sqrt{2}} = \frac{0.808 \times 350}{2\sqrt{2}} = 100V \quad (6)$$

The resulted voltage drop matches the voltage drop which is obtained from (4). Similar to Fig. 7, a compensating signal which corresponds to error voltage is generated and added to bus-clamping modulation signal in order to effectively compensate for the voltage drop.

To have accurate compensation strategy, the sampling delay of current sensing circuit is incorporated in dead-time com-

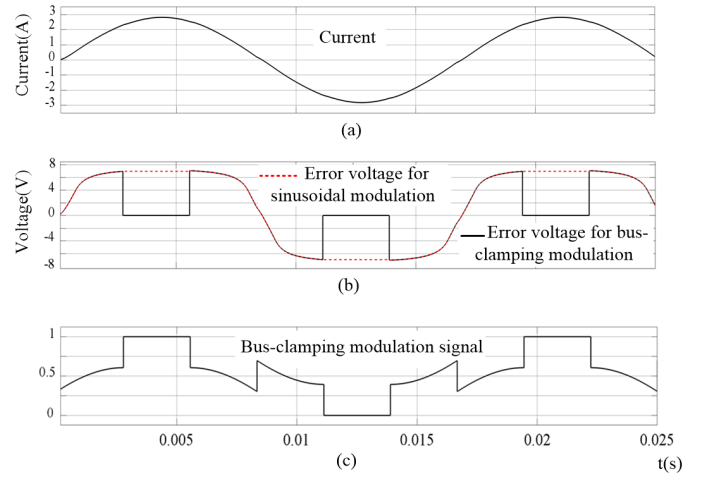


Fig. 9. The a) filtered phase current, b) the error voltage for sinusoidal and bus-clamping modulation signal and c) bus-clamping modulation signal.

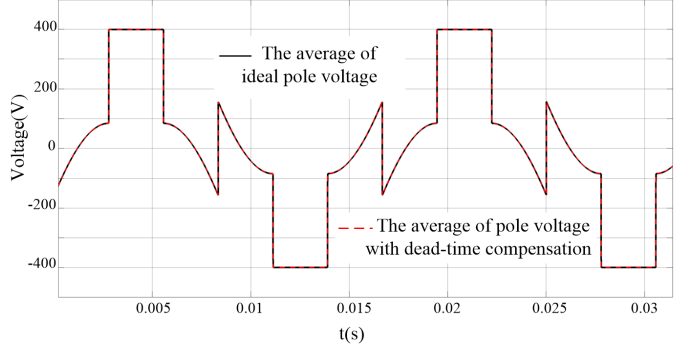


Fig. 10. The average of pole voltage in ideal case and after activation of dead-time compensation.

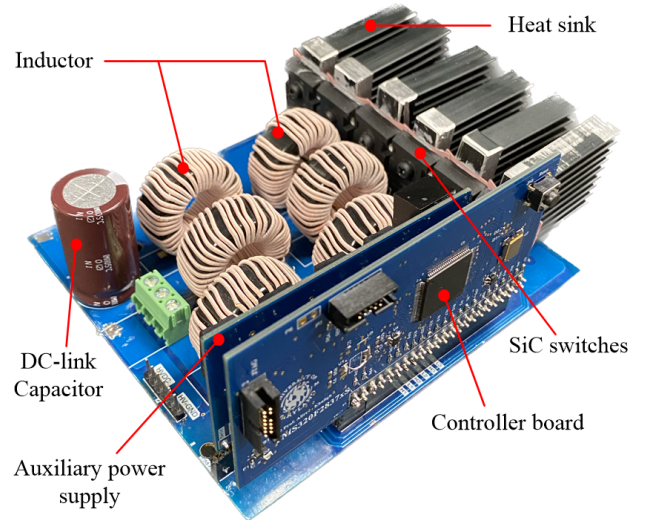


Fig. 11. Prototype for three phase VSI.

penation. The resulted output voltage after activation of dead-time compensation is illustrated in Fig. 12 (b) which reflects

TABLE II
THE PARAMETERS OF PROTOTYPE VSI CIRCUIT

Design Variable	Value
DC-link voltage	$V_{DC} = 350V$
Output phase voltage	$V_{ph} = 100V_{rms}$
Output line-to-line voltage	$V_{ph} = 173V_{rms}$
Switching frequency	$f_{sw} = 100kHz$
Output line frequency	$f_{line} = 60Hz$
Modulation index	$m = 0.808$
Dead-time	$t_{dT} = 300ns$
Switch C_{ds} capacitor	$C_{ds} = 68pF$
Switch part number	UJ4C075033K4S

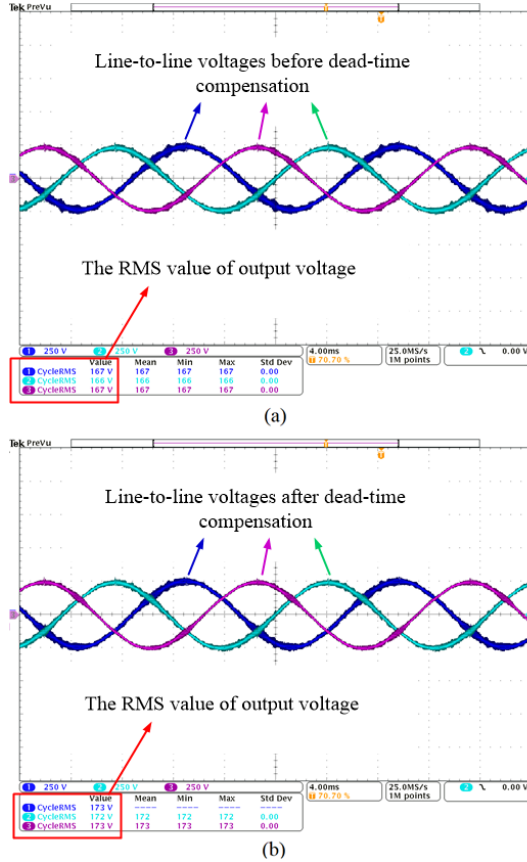


Fig. 12. The three-phase output line-to-line voltage a) before and b) after activating the dead-time compensation scheme.

173 Vrms line-to-line voltage that is matching the desired output voltage. Hence, the dead-time effect is accurately estimated using (4) and compensated according to Fig. 7.

V. CONCLUSION

This paper presented a method to compensate the error between actual and desired output voltage due to the effect of dead-time in bus-clamping PWM modulated VSI circuit. As

well as dead-time, the effect of drain-to-source capacitors C_{ds} of switches are considered in this analysis. First, the operation principle for switching transition of half bridge is analyzed to indicate the error between actual and intended output voltage which is introduced due to dead-time effect under different current directions. Subsequently, the error voltage is analyzed for a VSI which is modulated with bus-clamping technique to reduce the switching loss. The simulation results are provided to prove the effects of dead-time and C_{ds} capacitors on the output voltage drop. In order to verify the operation of compensation method experimentally, a three-phase VSI prototype is implemented. Based on experimental results, the presence dead-time and parasitic C_{ds} capacitors cause drop in desired output voltage RMS value. By activating the dead-time compensation method, the voltage drop is compensated and the output voltage matches the desired voltage for the applied modulation index value.

REFERENCES

- [1] J. Ye, Y. Huang, S. Huang, H. Wang, B. Li, J. Xu, and A. Shen, "An accurate dead time compensation method for spwm voltage source inverters," *IEEE Transactions on Power Electronics*, vol. 38, no. 4, pp. 4894–4908, 2022.
- [2] O. Rezaei, O. Mirzapour, M. Panahzari, and H. Gholami, "Hybrid ac/dc provisional microgrid planning model considering converter aging," *Electricity*, vol. 3, no. 2, pp. 236–250, 2022.
- [3] R. Ren, F. Zhang, B. Liu, F. Wang, Z. Chen, and J. Wu, "A closed-loop modulation scheme for duty cycle compensation of pwm voltage distortion at high switching frequency inverter," *IEEE Transactions on Industrial Electronics*, vol. 67, no. 2, pp. 1475–1486, 2019.
- [4] M. Salehi and M. Amirabadi, "A soft-switching zeta-based ac-link universal converter," in *2023 IEEE Applied Power Electronics Conference and Exposition (APEC)*, 2023, pp. 3233–3239.
- [5] M. A. Dashtaki, H. Nafisi, E. Pouresmaeil, and A. Khorsandi, "Virtual inertia implementation in dual two-level voltage source inverters," in *2020 11th Power Electronics, Drive Systems, and Technologies Conference (PEDSTC)*, 2020, pp. 1–6.
- [6] C. Roy, N. Kim, D. Evans, A. P. Sirat, J. Gafford, and B. Parkhideh, "A half-bridge on-state voltage sensor for in-situ measurements," in *2022 IEEE Energy Conversion Congress and Exposition (ECCE)*, 2022, pp. 1–7.
- [7] A. P. Sirat, H. Niakan, D. Evans, J. Gafford, and B. Parkhideh, "Ultra-wideband unidirectional reset-less rogowski coil switch current sensor topology for high-frequency dc-dc power converters," in *2023 IEEE Applied Power Electronics Conference and Exposition (APEC)*, 2023, pp. 1662–1669.
- [8] Y. Yang, K. Zhou, H. Wang, and F. Blaabjerg, "Analysis and mitigation of dead-time harmonics in the single-phase full-bridge pwm converter with repetitive controllers," *IEEE Transactions on Industry Applications*, vol. 54, no. 5, pp. 5343–5354, 2018.
- [9] A. Kulkarni, A. Gupta, and S. K. Mazumder, "Resolving practical design issues in a single-phase grid-connected gan-fet-based differential-mode inverter," *IEEE Transactions on Power Electronics*, vol. 33, no. 5, pp. 3734–3751, 2017.
- [10] D. Sandeep, P. Srikanth, B. S. Praneeth, J. Peter, and S. Athikkal, "Investigations on space vector based bus clamping pwm strategies on speed control of induction motor drive," in *2019 International Conference on Power Electronics Applications and Technology in Present Energy Scenario (PETPES)*. IEEE, 2019, pp. 1–6.
- [11] R. Rezaii, M. Nilian, R. Khalili, M. Safayatullah, and I. Batarseh, "A hybrid bidirectional dc-dc converter for electric vehicles applications," in *2022 IEEE International Conference on Industrial Technology (ICIT)*, 2022, pp. 1–6.
- [12] N. Souiri, S. Farhangi, H. Iman-Eini, and H. Ziar, "Modeling and estimation of the maximum power of solar arrays under partial shading conditions," in *2020 11th Power Electronics, Drive Systems, and Technologies Conference (PEDSTC)*, 2020, pp. 1–6.